



This is the accepted manuscript made available via CHORUS. The article has been published as:

# Upper limit on shift current generation in extended systems

Liang Z. Tan and Andrew M. Rappe

Phys. Rev. B **100**, 085102 — Published 1 August 2019

DOI: [10.1103/PhysRevB.100.085102](https://doi.org/10.1103/PhysRevB.100.085102)

# Upper limit on shift current generation in extended systems

Liang Z. Tan<sup>1</sup> and Andrew M. Rappe<sup>2</sup>

<sup>1</sup>*Molecular Foundry, Lawrence Berkeley National Laboratory, Berkeley, California 94720, United States*

<sup>2</sup>*Department of Chemistry, University of Pennsylvania, Philadelphia, Pennsylvania 19104, USA*

Despite a long history of research into nonlinear response theory, there has been no systematic investigation into the maximum amount of nonlinear optical response attainable in solid-state materials. In this work, we present an upper bound on the second-order response functions of materials, which controls the shift current response. We show that this bound depends on the band gap, band width, and geometrical properties of the material in question. We find that delocalized systems generally have larger responses than more localized or isolated ones. As a proof of principle, we perform first-principles calculations of the response tensors of a wide variety of materials, finding that the materials in our database do not yet saturate the upper bound. This suggests that new large shift current materials will likely be discovered by future materials research guided by the factors mentioned in this work.

The response functions of a material characterize its behavior under external stimuli, such as electromagnetic radiation. Such responses may grow linearly with the amplitude of the incident radiation, as is the case of absorption, or may be nonlinear. The latter category includes a diverse set of phenomena such as second harmonic generation (SHG) [1], shift current [2–5], sum frequency generation [6], and excited state absorption [7], among others. It is often desirable to generate large nonlinear optical effects, from the point of view of fundamental science, or for use in practical applications. While there has been the occasional discovery of materials with large nonlinear responses, the materials properties limiting the magnitude of these effects is not currently well understood.

In this paper, we treat the shift current bulk photovoltaic effect, which is the generation of current in a bulk single-phase material under illumination, and is a second order nonlinear optical effects. The induced current ( $J$ ) is proportional to the second power of the electric field ( $E$ ) of the incident light,

$$J_r(\omega_{\text{out}} = 0) = \sigma_{rst}^{\text{SC}}(\omega_{\text{in}}) E_s(\omega_{\text{in}}) E_t(-\omega_{\text{in}}) \quad (1)$$

where  $\omega_{\text{in}}$  is the frequency of the incident light, and  $\omega_{\text{out}}$  is the frequency of the response. As a result [3, 4], the shift current is present only in materials lacking inversion symmetry. The shift photocurrent can therefore be generated without the need for a traditional  $p$ - $n$  junction, which has motivated the field of ferroelectric photovoltaics [2, 5, 8–10].

In extended systems, the second order perturbation theory expressions for the shift current is [3, 11]

$$\sigma_{rst}^{\text{SC}}(\omega_{\text{in}}) = \pi e \left( \frac{e}{m\hbar\omega_{\text{in}}} \right)^2 \sum_{cv\vec{k}} \langle c\vec{k} | p_r | v\vec{k} \rangle \langle v\vec{k} | p_s | c\vec{k} \rangle \delta(\omega_c - \omega_v - \omega_{\text{in}}) \mathcal{R}_{rt}(c, v, \vec{k}) \quad (2)$$

Here, the sum over states includes all conduction ( $c$ ) and valence ( $v$ ) bands and corresponding integrals over the

Brillouin zone. The components of the momentum operator are denoted by  $p_r$ . The shift vector

$$\mathcal{R}_{rt}(c, v, \vec{k}) = -\frac{\partial}{\partial k_t} \arg \langle c\vec{k} | p_r | v\vec{k} \rangle - [\chi_{vt}(\vec{k}) - \chi_{ct}(\vec{k})] \quad (3)$$

contains the Berry connections ( $\chi$ ), and has been linked to topological ideas in nonlinear optics [12–14]. The shift vector  $\mathcal{R}$  can be understood as a generalized gauge invariant  $k$ -space derivative of the  $p$  operator [11, 15], and it is odd under the interchange of  $c$  and  $v$  bands. This formalism has been successfully used in first-principles calculations of shift current [5, 16, 17].

Second harmonic generation (SHG) is a closely related second-order effect with a response  $\omega_{\text{out}} = 2\omega_{\text{in}}$  instead of  $\omega_{\text{out}} = 0$ . The real part of the SHG nonlinear conductivity is

$$\begin{aligned} \text{Re } \sigma_{rst}^{\text{SHG}}(\omega_{\text{in}}) = & \pi e \left( \frac{e}{m\hbar\omega_{\text{in}}} \right)^2 \sum_{cv\vec{k}} \langle c\vec{k} | p_r | v\vec{k} \rangle \langle v\vec{k} | p_s | c\vec{k} \rangle \\ & \left( -\delta(\omega_c - \omega_v - \omega_{\text{in}}) + \frac{1}{2} \delta(\omega_c - \omega_v - 2\omega_{\text{in}}) \right) \\ & \mathcal{R}_{rt}(c, v, \vec{k}) \end{aligned} \quad (4)$$

Because of the similarities between Eqs. 2 and 4, most of the following results will also apply to the real part of SHG conductivity with some modification.

In applications of shift current, the quantity of interest is often not the value of the response function at a fixed frequency, but rather the values it takes across a range of frequencies. For instance, the total current produced by a photovoltaic device is given by the integral of  $\sigma(\omega_{\text{in}})$  weighted by the radiation intensities at all incident frequencies. Alternatively, one may be interested in the average response of a material across a frequency range instead of some predetermined frequency. We therefore use the integral  $M = |\int \sigma dE|$  as a metric for evaluating the overall magnitude of the nonlinear response of a material [18], where  $E = \hbar\omega$ . For the frequency range of this integral, we consider contributions

from the lowest conduction and highest valence bands of the material. This is therefore a metric for the lower frequency range of the nonlinear optical spectrum of a material. Having a large value of  $M$  does not necessarily mean that the nonlinear response is large over the entire Brillouin zone. Instead, the response can often be concentrated in hot spots [19]. Despite the truncation of Eqs. 2, 4 to two bands, it should be stressed that the bounds derived below are not the bounds of a purely two-level model system, but are bounds for the lowest two levels of a multi-level system. The difference is that the second-order susceptibility for a pure two-level system vanishes [20], whereas higher energy bands are taken into account even in the two lowest levels of Eqs. 2, 4 via the application of a sum rule [11].

We therefore consider the quantity (including a factor of 2 for spin degeneracy of bands)

$$M = \frac{2\pi e^3}{m^2 \hbar \omega_{\text{in}}^2} \left| \sum_{\vec{k}} \langle c\vec{k} | p_r | v\vec{k} \rangle \langle v\vec{k} | p_s | c\vec{k} \rangle \mathcal{R}_{rt}(c, v, \vec{k}) \right| \quad (5)$$

as a measure of the overall magnitude of shift current responses. For the real part of  $\sigma^{\text{SHG}}$ , we use  $M^{\text{SHG}} = M/2$ , with the additional factor of 1/2 arising from Eq. 4. SHG is often measured in terms of the nonlinear susceptibility, which is related to the nonlinear conductivity by  $\chi^{(2)} = \sigma^{\text{SHG}}/(2i\omega\epsilon_0)$ .

We begin our derivation of an upper bound on  $M$  by considering the Hamiltonian of the  $c$  and  $v$  bands, which determines the quantities appearing in Eq. 5. A generic Hamiltonian for this two band system (which may be obtained, for instance, through the use of maximally localized Wannier functions [21–23]) can be written as

$$H(\vec{k}) = \vec{h}(\vec{k}) \cdot \vec{\tau} = \sum_{i=1}^3 h_i(\vec{k}) \tau_i \quad (6)$$

where the  $\tau_i$  are Pauli matrices representing the band degree of freedom. The shift current of such a Hamiltonian was derived in [24]. For simplicity, we focus here on the longitudinal tensor components of the nonlinear response functions,  $\sigma_{iii}$  along some direction  $\vec{v}$ . With the above assumptions, our metric for the overall shift current magnitude becomes

$$M = \frac{\pi e^3}{2\hbar} \left| \int \frac{d^3k}{(2\pi)^3} \frac{\vec{h}(\vec{k}) \cdot \vec{h}'(\vec{k}) \times \vec{h}''(\vec{k})}{E(\vec{k})^3} \right| \quad (7)$$

where the derivatives  $\vec{h}' = \frac{d}{dk}\vec{h}$ ,  $\vec{h}'' = \frac{d^2}{dk^2}\vec{h}$  are taken along the direction of light polarization and current  $\vec{v}$ , and  $E(\vec{k}) = 2|\vec{h}(\vec{k})|$  is the band transition energy at  $\vec{k}$ . From the appearance of  $E(\vec{k})$  in the denominator of this expression, it can already be seen that small band gaps tend to favor large nonlinear responses, as has been noted in [25]. This, however, does not mean that minimizing the band energy throughout the entire Brillouin zone would yield the greatest possible response, because of the competing factors of  $\vec{h}'$  and  $\vec{h}''$  in the numerator, which favor variation in the Hamiltonian. In other words, dispersive bands would also tend to increase the amount of response. We therefore expect that a balance of these two factors determines the amount of response.

In a system with a fixed band gap, a rescaling of the band width will increase the value of  $\vec{h}''$ , and hence of  $M$ , without bound. In real materials, the Hamiltonian is restricted to physically attainable values. In the tight-binding picture, the band width grows with the strength of the hopping between atomic sites. We therefore impose the restriction that the Fourier components of  $\vec{h}$ , which are the hopping amplitudes between Wannier functions [21], are bounded in magnitude and decay exponentially with distance

$$\begin{aligned} \vec{h}(\vec{k}) &= \sum_{n_1 n_2 n_3} \vec{h}_{n_1 n_2 n_3} \exp(i\vec{k} \cdot (n_1 \vec{R}_1 + n_2 \vec{R}_2 + n_3 \vec{R}_3)) \\ |\vec{h}_{n_1 n_2 n_3}| &< A \exp\left(-\frac{n_1}{\xi_1} - \frac{n_2}{\xi_2} - \frac{n_3}{\xi_3}\right) \end{aligned} \quad (8)$$

Here,  $A$  is the overall scale for the magnitude of the Hamiltonian and  $\xi_i$  are the hopping ranges which can be different along different lattice directions  $\vec{R}_i$ . Since  $\vec{h}'$  and  $\vec{h}''$  scale with  $A$ , and transitions  $E(\vec{k})$  are no less than the band gap  $E_g$ , the form of Eq. 7 suggests that an upper bound for  $M$  is proportional to  $(A/E_g)^2$ . To derive a general upper bound, we proceed by bounding the product  $\vec{h}_{n'_1 n'_2 n'_3} \cdot \vec{h}_{n_1 n_2 n_3} \times \vec{h}_{n'_1 n'_2 n'_3} < |\vec{h}_{n'_1 n'_2 n'_3}| |\vec{h}_{n_1 n_2 n_3}| |\vec{h}_{n'_1 n'_2 n'_3}|$  and the energy denominator  $\mathcal{F}[1/|\vec{h}(\vec{k})|^2] < 4/E_g^2$  [26]. Using these inequalities and Eq. 8 in Eq. 7, we find

$$M < \frac{2\pi e^3}{\hbar} \left( \frac{A}{E_g} \right)^2 \Xi \left( \overset{\leftrightarrow}{R}, \vec{\xi}, \vec{v} \right) \quad (9)$$

where  $\Xi \left( \overset{\leftrightarrow}{R}, \vec{\xi}, \vec{v} \right)$  is a dimensionless geometrical factor depending on the crystal lattice ( $\overset{\leftrightarrow}{R} = (\vec{R}_1, \vec{R}_2, \vec{R}_3)$ ), hopping ranges ( $\vec{\xi}$ ), and the measurement direction  $\vec{v}$ . This bound holds for all non-zero values of  $A$ ,  $E_g$ , and  $\xi$ . The detailed form of the geometrical factor is

$$\Xi(\vec{R}, \vec{\xi}, \vec{v}) = \frac{1}{V} \left[ \sum_{i,j,l=(1\ 2\ 3)} \tilde{v}_i \frac{2e^{-1/\xi_i}}{(1-e^{-1/\xi_i})^2} \frac{1+e^{-1/\xi_j}}{1-e^{-1/\xi_j}} \frac{1+e^{-1/\xi_l}}{1-e^{-1/\xi_l}} \right. \\ \left. + \sum_{i,j,l=(1\ 2\ 3)} \tilde{v}_i^2 \frac{2(e^{-1/\xi_i} + e^{-2/\xi_i})}{(1-e^{-1/\xi_i})^3} \frac{1+e^{-1/\xi_j}}{1-e^{-1/\xi_j}} \frac{1+e^{-1/\xi_l}}{1-e^{-1/\xi_l}} + 2\tilde{v}_i\tilde{v}_j \frac{2e^{-1/\xi_i}}{(1-e^{-1/\xi_i})^2} \frac{2e^{-1/\xi_j}}{(1-e^{-1/\xi_j})^2} \frac{1+e^{-1/\xi_l}}{1-e^{-1/\xi_l}} \right] \quad (10)$$

Here, the volume of the unit cell is  $V = |\det R|$ , the sums run over all cyclic permutations of (1 2 3), and  $\tilde{v}_i = \sum_j R_{ji} v_j$ . This geometrical factor is an increasing function of the hopping ranges  $\vec{\xi}$ . The geometrical factor can vary greatly in magnitude depending on the range of hopping (Fig. 1), with the exact value depending on the shape of the unit cell and direction of measurement.  $\Xi$  is a rapidly growing function of the hopping ranges, asymptoting to  $\xi^9$  for large values of  $\xi$ . We therefore expect this factor to be large in materials where second- or higher-neighbor hopping is comparable to nearest neighbor hopping. Previous studies [5] have noted, based on observing trends in the calculated shift current across materials classes, that highly covalent materials with delocalized wavefunctions tend to have large shift currents. In the context of Eq. 9, we recognize two distinct, but related reasons for this trend. Firstly, materials with strong covalent bonds would have large hopping amplitudes  $A$ . Secondly, even if a material does not have particularly strong first-neighbor hopping, the presence of further-neighbor hopping comparable in magnitude would tend to delocalize wavefunctions and increase the geometrical factor  $\Xi$ . A further examination of Fig. 1 shows that highly asymmetric unit cells tend to increase  $\Xi$  as well, which is supported by the observation that some of the materials with highest predicted shift current contain 1-dimensional chains or motifs [27, 28].

We compare our derived bound Eq. 9 with ab-initio calculations in Fig. 2. We have selected a test set of 950 non-centrosymmetric materials from the MATERIALS PROJECT database [29], choosing those with less than 30 atoms per unit cell, for computational efficiency. We have restricted our calculations to non-magnetic materials, and to thermodynamically stable or metastable materials with decomposition energy of less than 0.1 eV/atom. These calculations were done with the PBE density functional [30], using norm-conserving RRKJ pseudopotentials [31], and using a planewave basis set with kinetic energy cutoff of 60 Ry. Spin-orbit coupling was included at the fully-relativistic level for all calculations. A Monkhorst-Pack  $16 \times 16 \times 16$   $k$ -point mesh was used for the self-consistent evaluation of the charge densities and calculation of the nonlinear response tensors. While these ab-initio calculations were performed at the level of density functional theory for computational efficiency, higher accuracy can be achieved by using quasiparticle-corrected quantities in the upper bound Eq. 9.

To make a direct comparison of ab-initio calculated response tensors to our analytical bound, we integrate

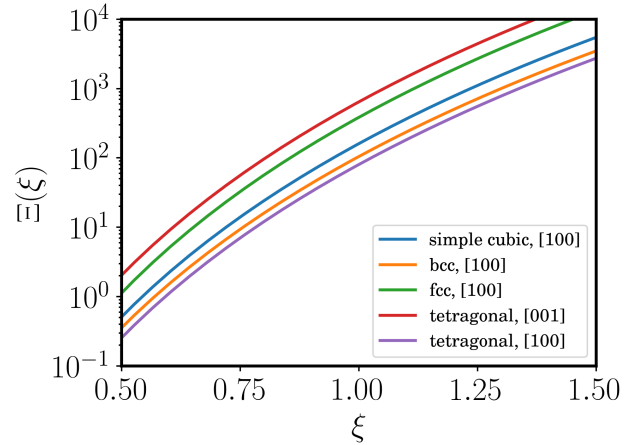


FIG. 1. Geometrical factor  $\Xi(\xi)$  for the upper bound on nonlinear optical response, as a function of the hopping range  $\xi$ , defined in Eq. 10 of the text. The geometrical factor is shown for different lattices, and for different measurement directions. Anisotropic lattices show the highest potential for large nonlinear responses. Here, the tetragonal lattice has  $c/a = 2.0$  ratio, and has largest nonlinear response upper limit for light polarization and current measurement directions along the  $c$ -axis.

the response tensors over an energy range corresponding to transitions between the lowest conduction band and highest valence band only. In Fig. 2, we plot, for each material, the largest tensor component of  $|\int \sigma dE|$ . Superimposed on the figure are contours corresponding to values of the bound (Eq. 9) at particular values of  $A$  and  $\Xi$ , with  $E_g$  allowed to vary. Most of the materials in the database fall below the contour with  $A=0.2$  eV and  $\Xi = 1$ . We note that the trend of the ab-initio data-points closely tracks the shape of the contours, with the materials with the largest responses having the smallest band gaps. Among these materials are the semimetals TaSe<sub>2</sub>, TaS<sub>2</sub>, Ca<sub>3</sub>Bi<sub>2</sub>O<sub>7</sub>, and LaAlGe. The experimentally measured SHG response of the Weyl semimetal TaAs was shown to be an order of magnitude larger than most other SHG materials [32]. The converse, however, is not true: having a small band gap does not necessarily mean that a material has large nonlinear response, as can be seen from Fig. 2. More generally, Eq. 9 is an upper bound rather than a correlation across the space of all materials.

In Fig. 2, there is a group of outliers which lie close

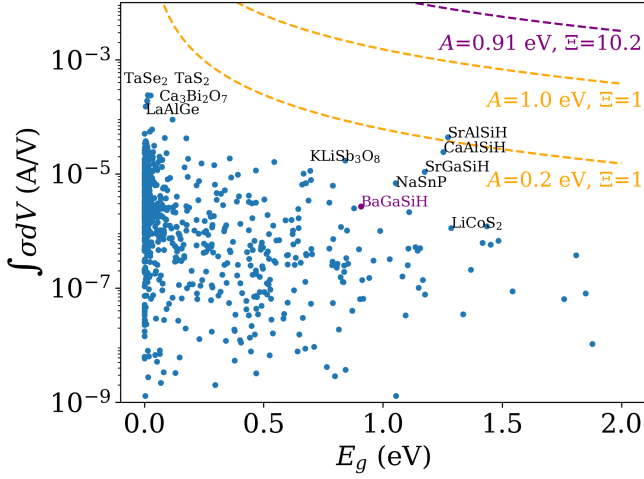


FIG. 2. Integrated nonlinear response for a test set of semiconductors and semimetals. The largest tensor component of the integrated nonlinear response for each material is plotted against the band gap. Dashed lines indicate the value of the nonlinear response upper bound (Eq. 9) as a function of the band gap, for different values of hopping strength ( $A$ ) and geometrical factor ( $\Xi$ ). Select materials with large responses (TaSe<sub>2</sub>, TaS<sub>2</sub>, Ca<sub>3</sub>Bi<sub>2</sub>O<sub>7</sub>, LaAlGe), or which deviate from the overall trend (SrGaSiH, SrAlSiH, CaAlSiH, NaSnP) are indicated on the plot. Shown in purple are the integrated nonlinear response of BaGaSiH and the theoretical bound constructed using the  $A$  and  $\Xi$  values of BaGaSiH.

to the  $A=0.2$  eV,  $\Xi = 1$  contour. This group contains several Zintl-type materials (AXYH, with  $A$ = group 1 or 2; X,Y=group 13–16). These materials are likely to have stronger or longer range bonding than other materials with the same band gap, and warrant further study into their photophysical properties. Among this group is BaGaSiH, with an integrated conductivity of  $M = 2.7 \times 10^{-6}$  A/V. We have constructed maximally localized Wannier orbitals from its frontier conduction and valence bands, and fitted the hopping parameters of the resulting Hamiltonian (Eq. 6) to an exponential dependence (Eq. 8), obtaining values of  $A = 0.91$  eV,  $\xi = 0.80$ ,  $\Xi = 10.12$ . The bound curve corresponding to the values of  $A$  and  $\Xi$  of BaGaSiH is shown in Fig. 2, indicating that the actual nonlinear response of BaGaSiH lies about three orders of magnitude below its theoretical bound. We compare this with BaTiO<sub>3</sub>, which is a prototypical ferroelectric with experimental data for bulk photocurrent [17, 33, 34]. Compared to BaGaSiH, BaTiO<sub>3</sub> has a smaller integrated response at  $M = 1.6 \times 10^{-7}$  A/V, and less delocalized bonding, with  $A = 0.53$  eV,  $\xi = 0.61$ ,  $\Xi = 0.64$ , which is also seen in the smaller spatial extent of its Wannier orbitals (Fig. 3).

The trend that delocalization of wavefunctions enhances shift current is in agreement with theoretical proposals [35, 36] and experimental observations in conjugated systems [37, 38]. With the hopping strength allowed to potentially increase to large values, these results

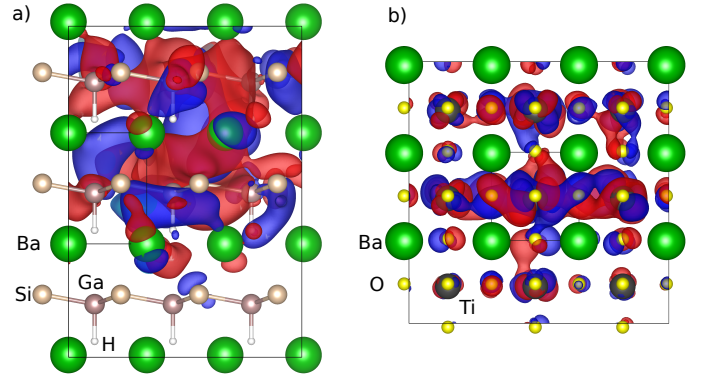


FIG. 3. Wannier functions constructed from frontier (conduction and valence) orbitals of (a) BaGaSiH and (b) BaTiO<sub>3</sub>. BaGaSiH is a large second harmonic generation and shift current material, with integrated response tensor (see text)  $\int \sigma d\omega = 2.7 \times 10^{-6}$  A/V. In contrast, BaTiO<sub>3</sub> has relatively low nonlinear response, with  $\int \sigma d\omega = 1.6 \times 10^{-7}$  A/V. These differences are explained in terms of the bonding character between the two materials. Isosurfaces of the Wannier functions of the two materials are plotted, with the isolevel chosen at 20% of the maximum value of the Wannier function. The Wannier orbitals of BaGaSiH ( $\xi = 0.80$ ,  $\Xi = 10.12$ ) are more diffuse than those of BaTiO<sub>3</sub> ( $\xi = 0.61$ ,  $\Xi = 0.64$ ), giving rise to longer range hopping in BaGaSiH.

indicate that Kuzyk's bound [39] for the SHG of isolated molecules can be broken by sufficiently delocalized systems. While only bulk materials were considered in our ab-initio database, the formalism of Eqs. 1–3 is general enough to include effects on the optical transition elements arising from heterogeneities such as point defects which could localize the wavefunctions and reduce the shift current.

In summary, we have derived a general upper limit for the shift current and second harmonic generation responses of extended systems, showing that it is controlled by the ratio of the hopping strength to the band gap of the material, as well as being dependent on a geometrical factor. These bounds may be used to guide materials research, by suggesting materials with potentially large responses, or as a screening tool to rule out unfavorable candidates. Besides the design of individual shift current materials, this work suggests that similar analytical relations may be found for other optical phenomena in solid state materials, such as second harmonic generation, high-order frequency mixing processes, multi-photon absorption, and Raman scattering.

## I. ACKNOWLEDGEMENTS

We thank Sai Lyu for discussions. L.Z.T. was supported by the U.S. ONR under Grant N00014-17-1-2574. A.M.R. was supported by the U.S. Department of Energy, under grant DE-FG02-07ER46431. Computational support was provided by the HPCMO of the U.S. DOD

- 
- [1] P. N. Prasad and D. J. Williams, *Introduction to non-linear optical effects in molecules and polymers* (Wiley, 1991).
- [2] V. Fridkin, A. Grekov, A. Rodin, E. Savchenko, and T. Volk, *Ferroelectrics* **6**, 71 (1973).
- [3] R. von Baltz and W. Kraut, *Phys. Rev. B* **23**, 5590 (1981).
- [4] V. I. Belinicher and B. I. Sturman, *Sov. Phys. USP.* **23**, 199 (1980).
- [5] L. Z. Tan, F. Zheng, S. M. Young, F. Wang, S. Liu, and A. M. Rappe, *npj Comp. Mater.* **2**, 16026 (1 (2016)).
- [6] Y. R. Shen, *Nature* **337**, 519 (1989).
- [7] Q. Bellier, N. S. Makarov, P.-A. Bouit, S. Rigaut, K. Kamada, P. Feneyrou, G. Berginc, O. Maury, J. W. Perry, and C. Andraud, *Physical Chemistry Chemical Physics* **14**, 15299 (2012).
- [8] H. Huang, *Nature Photonics* **4**, 134 (2010).
- [9] Y. Yuan, Z. Xiao, B. Yang, and J. Huang, *J. Mater. Chem. A* **2**, 6027 (2014).
- [10] C. Paillard, X. Bai, I. C. Infante, M. Guennou, G. Geneste, M. Alexe, J. Kreisel, and B. Dkhil, *Advanced Materials* **28**, 5153 (2016).
- [11] J. E. Sipe and A. I. Shkrebtii, *Phys. Rev. B* **61**, 5337 (2000).
- [12] T. Morimoto and N. Nagaosa, *Science Advances* **2**, e1501524 (2016).
- [13] L. Z. Tan and A. M. Rappe, *Physical Review Letters* **116**, 237402 (2016).
- [14] N. Nagaosa and T. Morimoto, *Advanced Materials*, 1603345 (2017).
- [15] C. Aversa and J. E. Sipe, *Phys. Rev. B* **52**, 14636 (1995).
- [16] J. L. P. Hughes and J. E. Sipe, *Physical Review B* **53**, 10751 (1996).
- [17] S. M. Young and A. M. Rappe, *Phys. Rev. Lett.* **109**, 116601 (2012).
- [18] T. Rangel, B. M. Fregoso, B. S. Mendoza, T. Morimoto, J. E. Moore, and J. B. Neaton, *Phys. Rev. Lett.* **119**, 067402 (2017).
- [19] L. Z. Tan and A. M. Rappe, *Journal of Physics: Condensed Matter* **31**, 084002 (2019).
- [20] M. G. Kuzyk, J. Pérez-Moreno, and S. Shafei, *Physics Reports* **529**, 297 (2013).
- [21] N. Marzari and D. Vanderbilt, *Phys. Rev. B.* **56**, 12847 (1997).
- [22] N. Marzari, A. A. Mostofi, J. R. Yates, I. Souza, and D. Vanderbilt, *Reviews of Modern Physics* **84**, 1419 (2012).
- [23] J. Ibañez-Azpiroz, S. S. Tsirkin, and I. Souza, *Phys. Rev. B* **97**, 245143 (2018).
- [24] B. M. Fregoso, T. Morimoto, and J. E. Moore, *Phys. Rev. B* **96**, 075421 (2017).
- [25] A. M. Cook, B. M. Fregoso, F. d. Juan, S. Coh, and J. E. Moore, *Nature Communications* **8**, 14176 (2017).
- [26] See Supplemental Material at [URL will be inserted by publisher] for derivation of upper bound.
- [27] J. A. Brehm, S. M. Young, F. Zheng, and A. M. Rappe, *The Journal of chemical physics* **141**, 204704 (2014).
- [28] S. Liu, F. Zheng, and A. M. Rappe, *The Journal of Physical Chemistry C* **121**, 6500 (2017).
- [29] A. Jain, S. P. Ong, G. Hautier, W. Chen, W. D. Richards, S. Dacek, S. Cholia, D. Gunter, D. Skinner, G. Ceder, and K. A. Persson, *APL Materials* **1**, 011002 (2013).
- [30] J. P. Perdew, K. Burke, and M. Ernzerhof, *Phys. Rev. Lett.* **77**, 3865 (1 (1996)).
- [31] A. M. Rappe, K. M. Rabe, E. Kaxiras, and J. D. Joannopoulos, *Phys. Rev. B Rapid Comm.* **41**, 1227 (1990).
- [32] L. Wu, S. Patankar, T. Morimoto, N. L. Nair, E. Thewalt, A. Little, J. G. Analytis, J. E. Moore, and J. Orenstein, *Nature Physics* **13**, 350 (2016).
- [33] A. G. Chynoweth, *Phys. Rev.* **102**, 705 (1956).
- [34] W. T. H. Koch, R. Munser, W. Ruppel, and P. Wurfel, *Ferroelectrics* **13**, 305 (1976).
- [35] J. Zhou, M. G. Kuzyk, and D. S. Watkins, *Optics Letters* **31**, 2891 (2006).
- [36] U. B. Szafruga, M. G. Kuzyk, and D. S. Watkins, *Journal of Nonlinear Optical Physics & Materials* **19**, 379 (2010).
- [37] J. Pérez-Moreno, Y. Zhao, K. Clays, M. G. Kuzyk, Y. Shen, L. Qiu, J. Hao, and K. Guo, *Journal of the American Chemical Society* **131**, 5084 (2009).
- [38] B. J. Coe, J. Fielden, S. P. Foxon, B. S. Brunschwig, I. Asselberghs, K. Clays, A. Samoc, and M. Samoc, *Journal of the American Chemical Society* **132**, 3496 (2010).
- [39] M. G. Kuzyk, *Physical Review Letters* **85**, 1218 (2000).